

Q-Band Resonance Raman Enhancement of Fe–CO Vibrations in Ferrous Chlorin Complexes: Possible Monitor of Axial Ligands in *d* Cytochromes

Jie Sun,^{1a} Chi K. Chang,^{1b} and Thomas M. Loehr*,^{1a}

Department of Chemistry, Biochemistry, and Molecular Biology, Oregon Graduate Institute of Science and Technology, P.O. Box 91000, Portland, Oregon 97291-1000, and Department of Chemistry, Michigan State University, East Lansing, Michigan 48824

Received: November 4, 1996[®]

Resonance Raman (rRaman) spectroscopy has been used extensively in the studies of the heme chemistry of carbon monoxy adducts. In porphyrin systems, the axial ligand vibrational modes of the CO, $\nu(\text{Fe–CO})$ and $\nu(\text{CO})$, are enhanced with Soret excitation via an A-term (Franck–Condon) mechanism, but are not expected with Q excitation (B-term or vibronic mechanism). For the first time, these modes have been obtained with Q_y as well as Soret excitation in rRaman spectra of CO complexes of ferrous chlorins. The enhancement with Q_y excitation arises from an A-term mechanism of Raman scattering for these chlorins owing to their reduced molecular symmetry. Thus, in iron chlorins or other heme systems with reduced molecular symmetry, axial ligand vibrational modes may be enhanced with Q_y excitation if they are observed with Soret excitation in the corresponding iron porphyrins. These findings show rRaman spectroscopy to be exceptionally valuable in the study of chlorin chromophores with Q_y enhancement using red or orange-red excitation. Furthermore, the method appears to be selective for chlorin cofactors in proteins containing multiple heme centers such as cytochrome *bd* oxidase (see, for example, Sun; et al. *Biochemistry* **1995**, 35, 2403–2412). It has been known that $\nu(\text{Fe–CO})$ and $\nu(\text{CO})$ frequencies of CO complexes of iron porphyrins and heme proteins exhibit linear correlations, falling into distinct sets for complexes possessing the same fifth ligand (for example, Ray; et al. *J. Am. Chem. Soc.* **1994**, 116, 162–176). In this work, we have found that $\nu(\text{Fe–CO})$ and $\nu(\text{CO})$ of iron-chlorin–CO complexes also respond to the nature of the opposite axial ligand and follow the same correlations derived from porphyrin systems. Thus, the reduction of one of the pyrrole rings of porphyrins has little effect on $\nu(\text{Fe–CO})$ and $\nu(\text{CO})$ frequencies, and their correlation behavior may perhaps be used to ascertain the identity of the proximal ligand of the chlorin in a protein system of unknown coordination, as in cytochrome *bd* oxidase.

Introduction

Interest in metallochlorins stems from the identification of dihydroxyprotochlorin as the cofactor for *d* hemes in cytochrome *bd* oxidase of *Escherichia coli*^{2–4} and *Azotobacter vinelandii*.^{5,6} The macrocycle structures of the *E. coli* (HP11) and *Penicillium vitale* catalases have recently been established as a *cis*-hydroxychlorin γ -spirolactone, formed with the 13-propionate side chain.⁷ A related hydroporphyrin is also believed to be in *Neurospora crassa* catalase.⁸ Another type of saturated porphyrin exists in sulfmyoglobins, where the pyrrole ring bearing the 8-vinyl group is saturated and possesses an exocyclic thiolene ring.⁹

Resonance Raman (rRaman) spectroscopy is a powerful structural probe of these dihydroporphyrins.^{10–15} Early analyses of metallochlorins depended on the analogy to those of well-studied metalloporphyrins and consideration of their reduced molecular symmetry.^{3,10,11,16} Later, independent normal coordinate analyses of metallochlorins were pursued.^{17–19} However, rRaman studies of iron chlorins are still rather limited relative to those of hemes in proteins and model systems. In particular, the enhancement behavior upon excitation in different regions of the chlorin absorption spectrum has not been systematically explored and is not fully understood. Only few iron chlorins have been investigated with red excitation.^{13–15,20,21} Thus, it is still an open question which rRaman modes would be

enhanced with red excitation, especially for the more complex *d* chromophores found in biological samples. Metallochlorins typically have a Q_y absorption band at ~ 600 – 650 nm having about one-third the intensity of the dominant Soret absorbance. In contrast, the Q bands of metalloporphyrins are blue-shifted by ~ 100 nm and are much weaker, being about one-tenth of the Soret intensity. The strong absorbance of metallochlorins allows the acquisition of high-quality rRaman spectra with red or orange-red excitation lines, thus offering a unique advantage in the study of metallochlorins. The understanding of red excitation rRaman spectra of biological heme *d* chromophores has been impaired by the lack of adequate model studies. For some heme *d* proteins, such as cytochrome *bd* oxidase (containing both *b* and *d* chromophores), the rRaman bands of heme *d* are only observed with red excitation by a selective enhancement mechanism. The observation of endogenous and/or exogenous metal–axial ligand vibrations with red excitation lines is of critical importance in identifying axial ligands of heme *d* and in probing the molecular and electronic structure of the ligand and the ligand-binding pocket.^{13–15,20}

Carbon monoxide has been used widely as a structural probe of the heme pocket environment. CO complexes of heme proteins and model compounds have been examined extensively by rRaman spectroscopy. An important discovery was the inverse linear relationship between $\nu(\text{CO})$ and $\nu(\text{Fe–CO})$.^{22–25} Furthermore, the classes of heme proteins with different proximal ligands (e.g., histidine, cysteine, ...) form their own individual negative linear correlations in a $\nu(\text{CO})$ vs $\nu(\text{Fe–CO})$ plot. If Fe–CO and CO frequencies are determined for a heme

* Author to whom correspondence should be addressed; e-mail (loehr@admin.ogi.edu), FAX (503)-690-1464.

[®] Abstract published in *Advance ACS Abstracts*, February 1, 1997.

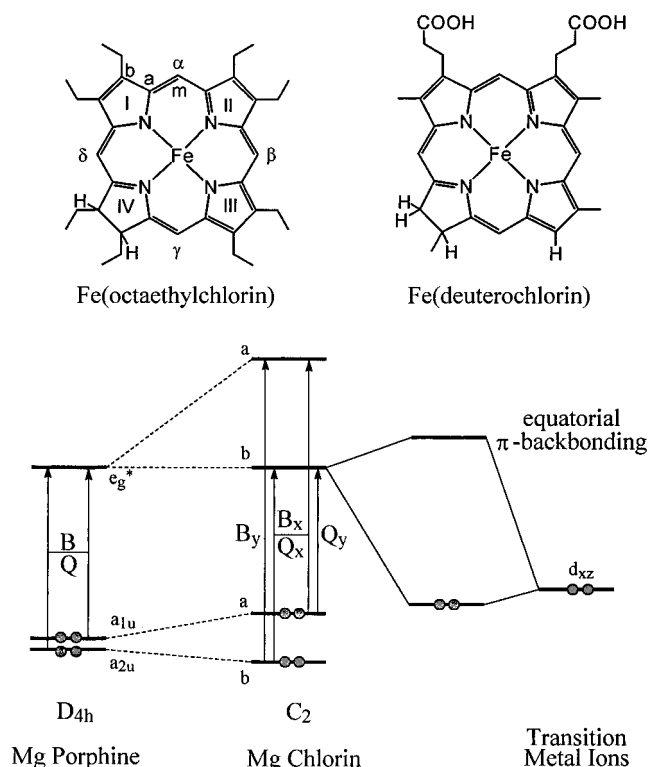


Figure 1. (Top) Structural diagrams of octaethylchlorin and deuteriochlorin, indicating the labeling scheme of atoms and rings. Although ring IV is shown as the reduced pyrrole ring in DC, either ring III or IV may be reduced. (Bottom) Qualitative MO diagram of metallochlorins. The relative energy levels of Mg porphine and Mg chlorin are taken from ref 34; a_{2u} and a_{1u} (HOMO) are occupied orbitals and e_g^* is the LUMO. The allowed electronic transitions are indicated by arrows. Configuration interactions are marked by a horizontal line between electronic transitions. The interaction between the occupied transition metal $b(d_{xz})$ and the chlorin $b(e_g^*)$ orbital, the equatorial π -back-bonding, leads to a hypsochromic shift of the Q_y transition. An interaction between the $a(d_{yz})$ and $a(e_g^*)$ orbital also exists, but is less significant due to a much larger energy separation. The equatorial π -back-bonding can be reduced by competition from strong axial π -back-bonding ligands such as CO.

system of unknown classification, the identity of the proximal ligand can be inferred from such a plot.²⁶ The actual Fe—CO and CO frequencies are primarily determined by the trans effect of the proximal (fifth) ligand and secondarily by π -back-bonding from $Fe \rightarrow \pi^*_{CO}$. The effect of the saturated ring of a chlorin on the axial π -back-bonding has not been examined. It will be of interest to know whether such a porphyrin-based $\nu(CO)$ vs $\nu(Fe-CO)$ plot can be extended to chlorins; if so, it may prove to be very valuable for the identification of the proximal ligands in heme *d* proteins.

The purpose of this paper is 2-fold: first, to examine the bands enhanced in Q_y -excited rRaman spectra of metallochlorins, especially $\nu(Fe-CO)$, $\delta(Fe-C-O)$, and $\nu(CO)$ modes, and second, to determine whether the $\nu(CO)$ vs $\nu(Fe-CO)$ plots established for porphyrin complexes can be extended to metallochlorins. For this investigation, two generic chlorin compounds, octaethylchlorin (OEC)²⁷ and deuteriochlorin (DC), have been employed (Figure 1).

Experimental Procedures

Preparation of Samples. $Fe^{III}(OEC)Cl$ and $Fe^{III}(DC)Cl$ (hydrolyzed) were prepared according to published procedures.^{11,28} $Fe^{II}(OEC)(2-MeIm)$ was prepared by shaking 5 mL of an O_2 -free, 400 μM $Fe^{III}(OEC)Cl$ solution in 1% 2-MeIm in CH_2Cl_2 (Aldrich, spectrophotometric grade) with 0.7 mL of a

concentrated aqueous $Na_2S_2O_4$ solution. $Fe^{II}(DC)(2-MeIm)$ was made in a parallel way. Reduction of $Fe^{III}(OEC)Cl$ in THF (Aldrich, spectrophotometric grade) by $(Bu_4N)BH_4$ (Aldrich) yielded $Fe^{II}(OEC)(THF)$. The reduction processes were monitored by UV-vis spectroscopy. The transfer of $\sim 20 \mu L$ of the above solutions to septum-sealed Pasteur pipets containing CO led to the formation of $Fe^{II}(OEC)(2-MeIm)(CO)$, $Fe^{II}(DC)(2-MeIm)(CO)$, and $Fe^{II}(OEC)(THF)(CO)$, respectively. ^{13}CO gas (99%) was purchased from Cambridge Isotope Laboratories (Woburn, MA). The samples thus made were sealed and used directly for UV-vis and rRaman measurements. FT-IR measurements were made using an Ar-purged, rubber-stopper-sealed KBr cell (1-mm path length) filled with preformed CO complexes of the ferrous chlorins. All sample transfers were carried out under an Ar atmosphere using gastight syringes.

Spectroscopy. Optical absorption spectra were recorded on a Perkin-Elmer Lambda 9 spectrophotometer at a spectral band width of 2 nm with the sample capillary tubes placed in a black Delrin holder.²⁹ FT-IR spectra were measured on a Perkin-Elmer 2000 FT-IR/FT-Raman spectrometer with 4- cm^{-1} resolution. Resonance Raman spectra were obtained on a custom McPherson (Acton, MA) Model 2061/207 spectrograph operated at a focal length of 0.67 m and equipped with a Princeton Instruments (Trenton, NJ) LN1100PB CCD detector. Rayleigh scattering was attenuated by using a Kaiser Optical (Ann Arbor, MI) 413.1-nm notch filter or a McPherson Model 275 double monochromator as prefilter. Excitation sources (Coherent, Santa Clara, CA) consisted of an Innova 302 Kr laser (413.1 nm) or an Innova 90-6 Ar-laser-pumped 599-01 dye laser using rhodamine 6G (tuned to 612 nm). All laser lines were filtered through an Applied Photophysics (Leatherhead, U.K.) optical glass or quartz prism monochromator to remove plasma emissions. Spectra were collected in a 90°-scattering geometry from solution samples in glass capillary tubes cooled by a muffin fan. Spectral resolution was $\sim 5.5 \text{ cm}^{-1}$. CCl_4 was used as a standard for polarization. Indene and/or CH_3CN , $K_3Fe(CN)_6$, CCl_4 were used as the calibrants for the frequency shifts with the CCD spectrograph.

Results and Discussion

As seen from the crystal structure of $Fe(OEC)^{30}$ metallochlorins generally lose the planar ring structure of metalloporphyrins. Based on its pseudo- S_4 ruffled structure, Andersson et al.¹¹ assigned an effective $C_2(x)$ symmetry to metallochlorins, an assignment that has been used by later workers.^{16,31,32} This reduction of symmetry has a profound impact on UV-vis and vibrational spectra of metallochlorins.

A. Electronic Properties. The electronic absorption spectra of metallochlorins have been examined extensively.³³ Unlike their metalloporphyrin counterparts, these spectra exhibit a strong Q_y band at ~ 600 – 650 nm together with more intense B or Soret bands at ~ 400 nm owing to the diminished configuration interaction between porphyrin $a_{1u} \rightarrow e_g^*$ and $a_{2u} \rightarrow e_g^*$ transitions. In metalloporphyrins, a_{1u} and a_{2u} orbitals are very close in energy and can sometimes be reversed in order. Under the group C_2 for metallochlorins, the a_{1u} and a_{2u} orbital symmetries are reduced to a and b, and e_g^* is split into a and b. An *ab initio* calculation on Mg(chlorin) indicates that the $a(a_{1u}, \text{HOMO})$ and $b(a_{2u})$ energy levels are farther apart; the $b(e_g^*, \text{LUMO})$ orbital energy is unchanged, while that of the $a(e_g^*)$ is greatly elevated (Figure 1).³⁴ The two electronic transitions, $a(a_{1u}) \rightarrow b(e_g^*)$ and $b(a_{2u}) \rightarrow a(e_g^*)$, now have a much larger energy difference and, thus, substantially reduced configuration interaction. The result is the red-shift and intensification of the Q_y absorption band. The other two

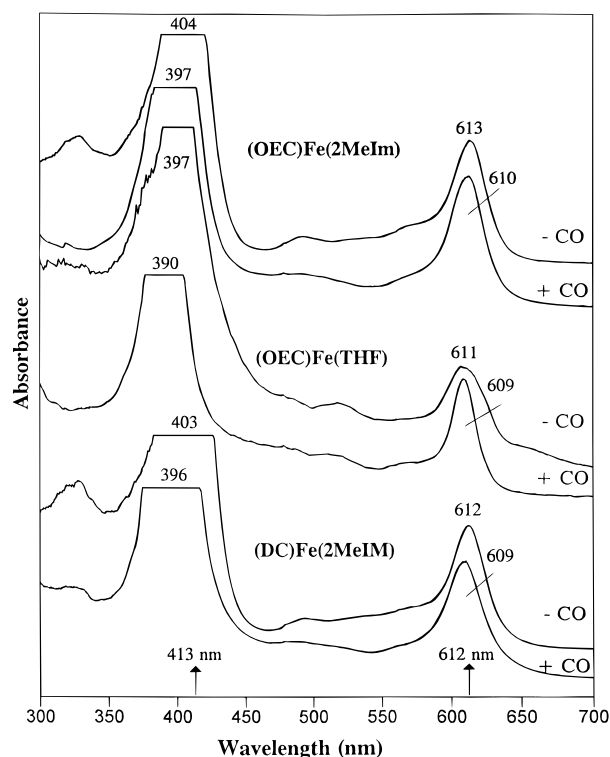


Figure 2. UV-vis spectra of Fe(OEC)(2-MeIm), Fe(OEC)(THF), and Fe(DC)(2-MeIm) in the absence and presence of CO. Soret absorptions are beyond the instrument limit (see text), and their maxima are estimates.

electronic transitions, $a(a_{1u}) \rightarrow a(e_g^*)$ and $b(a_{2u}) \rightarrow b(e_g^*)$, are similar in energy and, thus, have a behavior similar to those in metalloporphyrins with reduced total absorption intensity (B_x and Q_x). Consequently, the absorbance ratio Q_y/Soret is $\sim 1/3$ for metallochlorins, in contrast to $\sim 1/10$ for metalloporphyrins.^{33,35} This change in the absorption pattern also affects the rRaman spectra of metallochlorins. Prendergast and Spiro pointed out that Soret and Q_y excitation lead to Franck-Condon enhancement of the totally symmetric vibrational modes, whereas depolarized B-symmetry modes are best observed with Q_x excitation.¹⁸

The effect of transition metal d orbitals and axial ligands on chlorins can be explained qualitatively by analogy with metalloporphyrins.³⁵ The dominant interaction between metal and chlorin orbitals is the overlap between the d_{xz} and $b(e_g^*)$ orbitals, leading to equatorial π -back-bonding (Figure 1). This interaction yields a hypso shift of the Q_y absorption by elevating the $b(e_g^*)$ orbital energy relative to Mg(chlorin). However, this equatorial π -back-bonding can be reduced by competition with a strong axial π -acceptor ligand such as CO. Therefore, the blue-shifted Q_y band is expected to be at a lower energy when the axial ligand is CO than with a weaker π -back-bonder such as pyridine or imidazole. Because the energy level of $b(e_g^*)$ is almost the same as that of a metalloporphyrin e_g^* , the extent of equatorial π -back-bonding and the effect of an axial ligand are expected to be very similar to those of the porphyrin system.

The UV-vis spectra of Fe(OEC)(2-MeIm), Fe(DC)(2-MeIm), and Fe(OEC)(THF) in the absence and presence of CO are shown in Figure 2. These electronic spectra were recorded from the sealed cells prepared for the rRaman experiments, and their absorbances in the Soret region exceeded the instrument's upper limit. Despite this limitation, absorption maxima clearly show blue-shifts when CO is added, and this behavior parallels that of the corresponding iron porphyrin systems. The Q_y bands show smaller blue-shifts upon CO addition. The Q_y values of

the three CO adducts are all at ~ 609 nm and are comparable to those of Fe(OEC)(py)(CO) or Fe(OEC)(*N*-MeIm)(CO) (~ 609 nm), but are at longer wavelengths than those of Fe(OEC)(py)₂ or Fe(OEC)(*N*-MeIm)₂ (599 nm),³⁶ as anticipated.

B. Chlorin in-Plane Skeletal Vibrations. Although porphyrin skeletal normal modes are well established, there has been a controversy whether chlorin normal modes are significantly different from those of porphyrins. Bocian and co-workers advocated that chlorin normal modes are independent of those of porphyrins and emphasized that localized normal modes derive from the saturated ring (*cf.* Figure 1).^{17,19,32} In contrast, Prendergast and Spiro concluded that chlorin normal modes are not very different from those of porphyrins.¹⁸ Using meso $\alpha\beta$ -d₂ and $\gamma\delta$ -d₂ labeled OEC compounds, Fonda et al. have since shown experimentally that some chlorin modes are indeed localized. These authors stated that it is not possible to assign vibrational modes of metallochlorins by direct analogy with metalloporphyrins.³¹ However, in the important spectral region for many biological studies (1450–1700 cm^{-1}), only two modes show significant mode localization: 1613 cm^{-1} for Ni(OEC) and 1602 and 1543 cm^{-1} for Cu(OEC). These modes probably arise from the Raman-inactive modes ν_{37a} and ν_{38b} under D_{4h} symmetry of metalloporphyrins. Perhaps the most useful spin and coordination indicator bands for iron porphyrins are ν_3 and ν_{10} . In the Fe(OEC) systems, these modes show little localization.³¹ For example, upon $\alpha\beta$ -d₂ and $\gamma\delta$ -d₂ substitutions, ν_3 exhibits the same isotope shifts, whereas ν_{10} shows only a small difference. We also note that the ν_3 and ν_{10} frequencies for the iron chlorins are very similar to those of the corresponding iron porphyrins lying within ± 2 and ± 4 cm^{-1} , respectively. These facts show that the differences between the ν_3 and ν_{10} normal modes of iron porphyrins and chlorins are relatively minor. Other chlorin high-frequency modes such as ν_2 , ν_4 , ν_{11} , and ν_{19} also show similar correspondence between iron porphyrins and iron chlorins. Thus, we have again found it convenient to assign selected chlorin modes by comparison with well-established porphyrin-equivalent modes.^{11,14,15,37,38} Ambiguity may arise in assigning some bands because of the spectral congestion due to activation of ν_{37a} , ν_{37b} , ν_{38a} , ν_{38b} , ν_{41a} , and ν_{42} as well as vinyl modes in the case of heme *d* proteins. Such difficulties, however, are not expected for the relatively isolated ν_3 and ν_{10} bands. Given the fact that these latter modes are reliable indicators of the iron spin and coordination states in heme systems, it is practical to adapt them to metallochlorins rather than introducing a new nomenclature.

(1) CO Complexes of Ferrous Chlorins. Resonance Raman spectra of Fe(OEC)(2-MeIm)(CO) obtained with 413.1- and 612-nm excitation are shown in Figure 3. The compound is sensitive to laser irradiation at 413.1 nm. Even at 5 mW, bands of Fe(OEC)(2-MeIm) begin to emerge. However, the photodissociation of CO can be completely prevented by using even lower laser power of ~ 1 mW (Figure 3). No photosensitivity was observed with 612-nm excitation even with laser power as high as 50 mW. In 413- and 612-nm rRaman spectra, six bands are observed above 1450 cm^{-1} . The band at 1631 cm^{-1} is polarized and thus assigned to ν_{10} . No other polarized bands are expected near this frequency. The polarized band at 1497 cm^{-1} can be unambiguously assigned as the ν_3 mode. The depolarized band at 1464 cm^{-1} is tentatively assigned to ν_{28} and ν_{39b} . The polarized band at 1547 cm^{-1} is a candidate for ν_{11} or ν_{38a} . The band at 1581 cm^{-1} is depolarized and probably arises from ν_{19} or ν_{37b} . We assign the polarized band at 1597 cm^{-1} as ν_2 or ν_{37a} . Definitive assignments for the last four bands would require isotope-labeled OEC complexes and are beyond

TABLE 1: Skeletal Mode Frequencies of 6cLS CO Complexes of Ferrous Chlorins Compared with Carbon Monoxy Hemoglobin, and the Corresponding Parent 5cHS Ferrous Chlorins Compared with a Ferrous Porphyrin and Deoxymyoglobin

compounds	ν_2	ν_3	ν_4	ν_{10}	ν_{11}	ν_{19}	ref
6cLS CO complexes							
Fe(OEC)(2-MeIm)(CO)	1597 (p)	1497 (p)	1366 (p)	1631 (p)	1547 (p)	1581 (dp)	this work
Fe(OEC)(THF)(CO)	1604	1501	1365	1635	1553	1585	this work
Fe(DC)(2-MeIm)(CO)	1600	1495	1371	1628	~1548?	1587	this work
hemoglobin•CO	1586 ^a	1498	1372	1633	1556	n.d.	ref 46
5cHS complexes							
Fe(OEC)(2-MeIm)	1579 (p)	1474 (p)	1365 (p)	1606 (p)	1534 (p)	1559 (dp)	this work
Fe(OEC)(THF)	1579	1475	1365	1608 (p)	1534	1561	this work
Fe(DC)(2-MeIm)	1584 (p)	1470 (p)	1367	1607 (p)	1536 (p)	1564 (dp)	this work
Fe(OEP)(2-MeIm)	1581	~1474	1362	1608	n.d.	1551	ref 12
deoxymyoglobin	1563 ^a	1473	1357	1607	1546	?	ref 47

^a This normal mode has a different composition due to the presence of vinyl groups on the biological heme moiety.

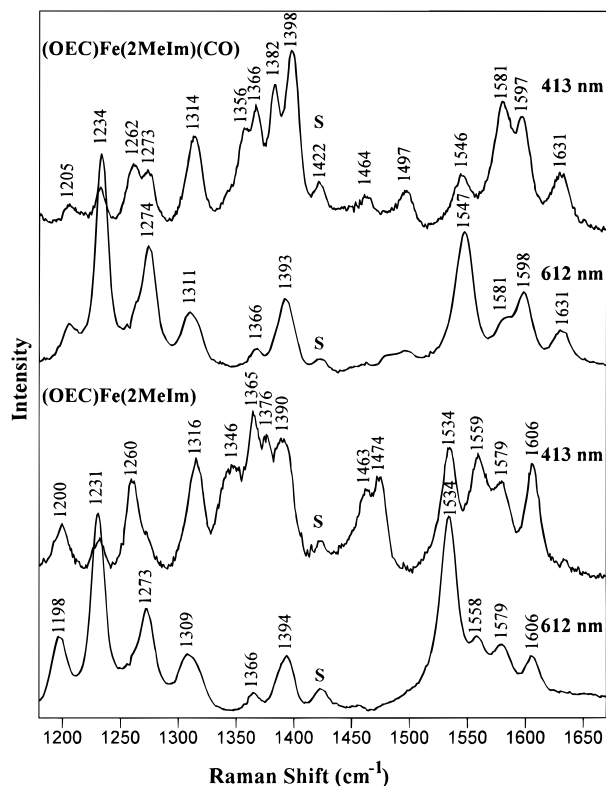


Figure 3. Resonance Raman spectra of Fe(OEC)(2-MeIm) in the presence and absence of CO. The laser power was 1 mW (413.1 nm) and 50 mW (612 nm) for Fe(OEC)(2-MeIm)(CO), and 5 mW (413.1 nm) and 50 mW (612 nm) for Fe(OEC)(2-MeIm).

the scope of the present investigation. Our proposed assignments are summarized in Table 1.

When the 2-MeIm axial ligand of Fe(OEC)(2-MeIm)(CO) is replaced by the weak-field THF ligand, all bands $> 1470 \text{ cm}^{-1}$ show 3- to 7- cm^{-1} increases in frequency (Figure 4). These increases may be explained by reduced equatorial π -back-bonding into the chlorin $b(e_g^*)$ orbital, as previously discussed.²⁵ The $b(e_g^*)$ orbital energy is almost identical to that of the porphyrin e_g^* according to the *ab initio* calculation on Mg(OEC)³⁴ and should be viewed as a combination of C_b-C_b antibonding, C_a-C_m antibonding, and C_a-C_b bonding. The observed frequency upshifts are consistent with significant contributions of C_a-C_m and/or C_b-C_b in these chlorin normal modes.¹⁸ Our assignments for Fe(OEC)(THF)(CO) are also included in Table 1.

The rRaman spectrum of Fe(DC)(2-MeIm)(CO) obtained with 413.1-nm excitation is shown in Figure 5. This compound is very sensitive to irradiation, its spectrum changing to that of the 5cHS Fe(DC)(2-MeIm) even with $\sim 2 \text{ mW}$ owing to

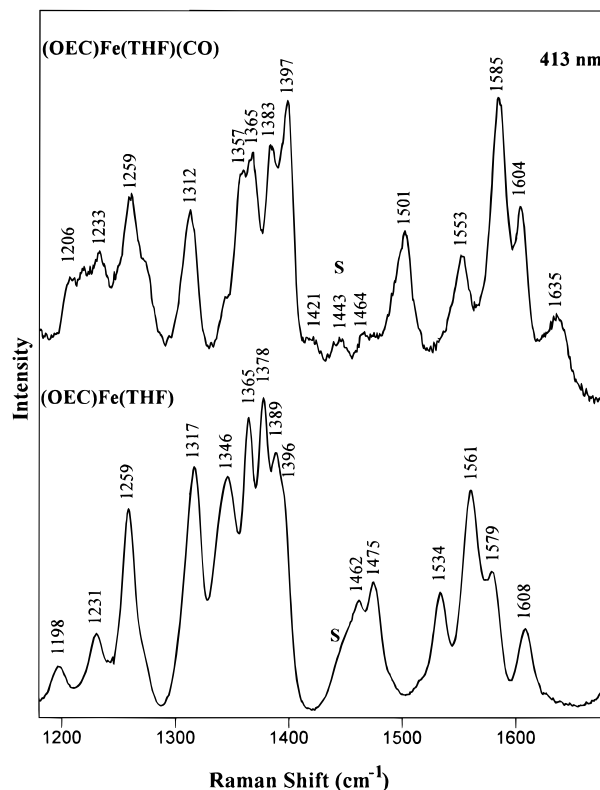


Figure 4. Resonance Raman spectra of Fe(OEC)(THF) in the presence and absence of CO. The laser power was 2 and 10 mW (at 413.1 nm) for Fe(OEC)(THF)(CO) and Fe(OEC)(THF), respectively.

photodissociation of CO. However, the dissociation is reversible: decreasing the incident power to $\sim 0.5 \text{ mW}$ restored the spectrum of the 6cLS CO complex. Although this spectrum is of lower quality, features similar to those of Fe(OEC)(2-MeIm)(CO) are obvious. For example, the ν_3 and ν_{10} bands are observed at 1495 and 1628 cm^{-1} , respectively. Band assignments for the DC complex are also listed in Table 1. No satisfactory rRaman spectra of the deuteriochlorin complexes could be obtained with 612-nm excitation owing to their high fluorescence at this wavelength.

(2) *5cHS Ferrous Chlorins.* Resonance Raman spectra of several 5cHS ferrous chlorin compounds, including sulfmyoglobin, have been studied previously, but usually only with near-Soret or Q_x excitation. Resonance Raman spectra of the 5cHS OEC and DC complexes described above obtained with Soret and Q_y excitation are also shown in Figures 3–5 together with the rRaman spectra of their corresponding CO complexes. Polarization analyses (spectra not shown) for Fe(OEC)(2-MeIm) (413.1- and 612-nm spectra) and for Fe(DC)(2-MeIm) (413.1 nm) facilitated spectral assignments.

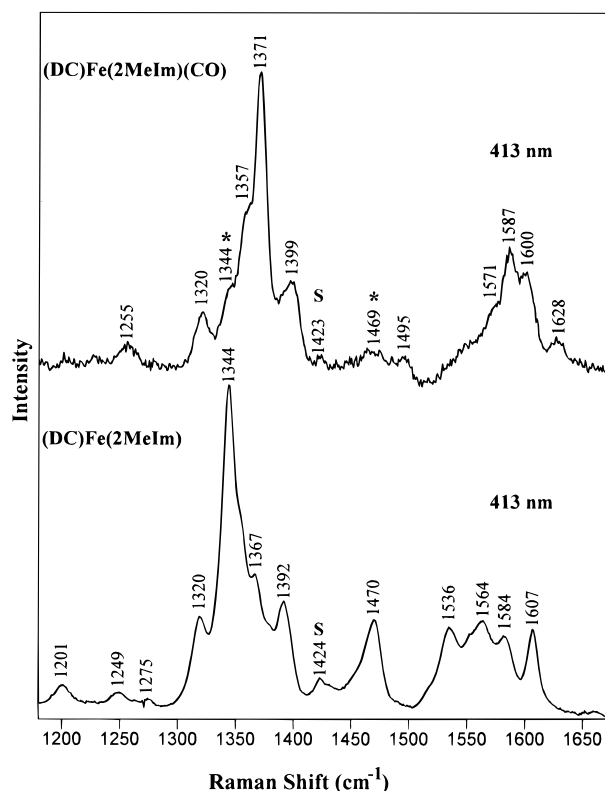


Figure 5. Resonance Raman spectra of Fe(DC)(2-MeIm) in the presence and absence of CO. The 413.1-nm laser power was 0.5 and 10 mW for Fe(DC)(2-MeIm)(CO) and Fe(DC)(2-MeIm), respectively.

The rRaman spectra of Fe(OEC)(2-MeIm) are dominated by polarized bands when using 413.1- and 612-nm excitation (Figure 3). A number of depolarized bands are observed at 1376, 1390, 1463, and 1559 cm^{-1} (413.1-nm spectrum) and 1309 and 1558 cm^{-1} (612-nm spectrum). The dominance of polarized bands and the activation of a strong band at 1231 cm^{-1} (ν_{42a}) in the Q_y rRaman spectrum represent the most significant departures from metalloporphyrin spectra. Other chlorin characteristics include the appearance of multiple bands near $\sim 1360\text{--}1370\text{ cm}^{-1}$ in the Soret rRaman spectrum as opposed to a single intense ν_4 porphyrin band. We assign the polarized bands at 1474 and 1606 cm^{-1} to ν_3 and ν_{10} , respectively. The band at 1463 cm^{-1} cannot be assigned to ν_3 since it is depolarized, and we attribute it to ν_{28} . It is worth noting that ν_{10} is enhanced in the Q_y -excited rRaman spectrum of Fe(OEC)(2-MeIm), whereas ν_3 is weak. Bands at 1579 (p), 1559 (dp), and 1534 cm^{-1} (p) may be identified with the porphyrin-equivalent ν_2 , ν_{19} , and ν_{11} modes. Tentative assignments for the 5cHS complexes are given in Table 1. As discussed above, these assignments are less definitive since alternative interpretations do exist.^{17,19}

The rRaman spectra of Fe(OEC)(THF) and Fe(DC)(2-MeIm) are shown in Figures 4 and 5, and their mode assignments are summarized in Table 1. A clear difference in the $\sim 1360\text{--}1370\text{ cm}^{-1}$ region of the Fe(DC)(2-MeIm) spectrum is its dominant peak at 1344 cm^{-1} in place of the more typical multiplet seen in the spectra of the Fe(OEC) complexes (Figures 3 and 4). The difference may arise from mode mixing: a number of A-symmetry bands such as ν_{29} , ν_{40a} , and ν_{41a} are expected in this region in addition to ν_4 . A normal coordinate analysis of Ni(OEC) indicates that some of these modes involve vibrations from substituent ethyl groups,¹⁷ which will be replaced by hydrogen atoms in DC. These normal modes would thus be slightly different between OEC and DC. It is interesting that reduced sulfmyoglobin exhibits an intensity pattern similar to

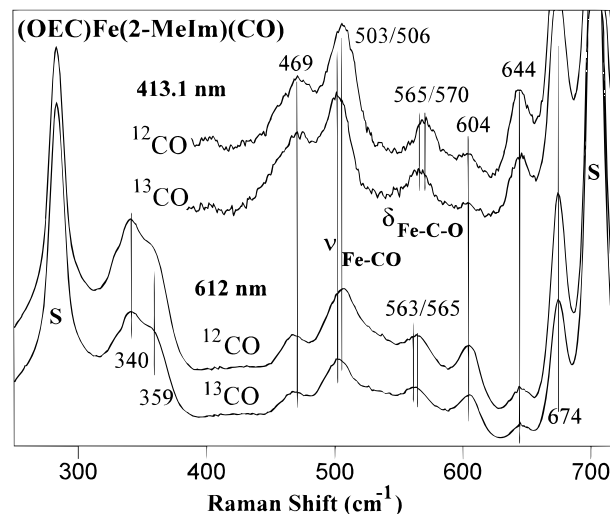


Figure 6. Low-frequency resonance Raman spectra of Fe(OEC)(2-MeIm)(CO) obtained with 413.1- and 612-nm excitation. The laser power was 1 mW (413.1 nm) and 50 mW (612 nm). The spectra of ^{12}CO and ^{13}CO samples were collected back-to-back under identical instrumental conditions.

that of Fe(DC)(2-MeIm). Because of its intensity, the 1344- cm^{-1} band of the reduced sulfmyoglobin was assigned to ν_4 .¹⁰ We now prefer to assign the band at 1367 cm^{-1} of Fe(DC)(2-MeIm) to ν_4 since its frequency is more similar to ν_4 values of other OEC compounds.

C. Identification of $\nu(\text{Fe-CO})$, $\nu(\text{CO})$, and $\delta(\text{Fe-C-O})$ Vibrations. The Fe-CO and CO stretching and Fe-C-O bending modes observed in the rRaman spectra of metalloporphyrin-CO complexes with Soret excitation are well documented.^{22–25} The A-term enhancement of $\nu(\text{Fe-CO})$ and $\nu(\text{CO})$ (A_1 under an effective C_{4v} symmetry) can be attributed to geometry differences in Fe-CO and CO bond distances between the ground and excited states.²⁵ The enhancement of $\delta(\text{Fe-C-O})$ (E symmetry) was first proposed to be an indicator of nonlinear CO-binding geometry.³⁹ It was pointed out recently that the loss of the 4-fold symmetry can be caused by an electrostatic interaction with the CO group.²⁵ Other workers suggested that the band assigned to $\delta(\text{Fe-C-O})$ is actually a combination mode.⁴⁰ None of the $\nu(\text{Fe-CO})$, $\nu(\text{CO})$, and $\delta(\text{Fe-C-O})$ modes is expected to be enhanced under Q-band excitation, where only vibronically active A_2 , B_1 , and B_2 modes are enhanced through a B-term mechanism. In metallochlorin-CO complexes, however, rRaman enhancement is operated by an A-term mechanism under both Soret and Q_y excitation and $\nu(\text{Fe-CO})$, $\nu(\text{CO})$, and $\delta(\text{Fe-C-O})$ modes are indeed observed with both 413- and 612-nm excitation, as detailed below. No symmetry reduction is required here for enhancement of the $\delta(\text{Fe-C-O})$ mode because the chlorin macrocycle possesses, at most, C_2 symmetry.

The low-frequency rRaman spectra of Fe(OEC)(2-MeIm)(CO) obtained with 413- and 612-nm laser lines are shown in Figure 6. The $\nu(\text{Fe-CO})$ and $\delta(\text{Fe-C-O})$ modes are identified by isotopic substitution with ^{13}CO . The CO stretching frequency is observed in FT-IR and rRaman (612 nm) spectra (Figure 7). In metalloporphyrin systems, these three modes show ^{13}C shifts of 2–7, 8–21, and 39–48 cm^{-1} , respectively. For Fe(OEC)(2-MeIm)(CO), the 506- cm^{-1} band shifts to 503 cm^{-1} with ^{13}CO in both 413- and 612-nm excitation spectra. The frequency and $\Delta(^{12}\text{CO}-^{13}\text{CO})$ values suggest that this band is the $\nu(\text{Fe-CO})$ mode. The weaker band at 570 cm^{-1} (413-nm spectrum) shifts to 565 cm^{-1} with ^{13}CO . We assign this band to $\delta(\text{Fe-C-O})$. In the 612-nm spectrum, however, this isotope-sensitive band is observed at 565 cm^{-1} ; the apparent difference may be

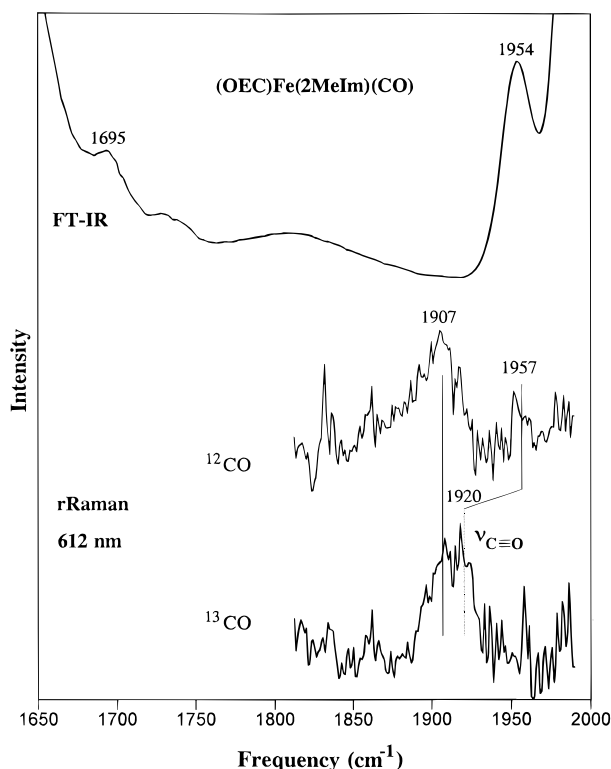


Figure 7. High-frequency FT-IR and resonance Raman (612 nm) spectra of Fe(OEC)(2-MeIm)(CO). Experimental conditions as in Figure 6.

due to overlap with a chlorin band. The presence of such a contributing chlorin band is suggested by the smaller isotope shift of 2 cm^{-1} compared to that ($\sim 5 \text{ cm}^{-1}$) with 413-nm excitation. In the CO stretching frequency region, we observe a ^{13}C -sensitive band at 1957 cm^{-1} in the 612-nm rRaman spectrum. Although its peak intensity is very weak, the corresponding intense IR band is observed at 1954 cm^{-1} . The Raman band shifts to $\sim 1920 \text{ cm}^{-1}$ in the ^{13}CO sample, overlapping with a nearby 1907- cm^{-1} band.

The low-frequency rRaman data for Fe(OEC)(THF)(CO) and Fe(DC)(2-MeIm)(CO) and their ^{13}CO isotopomers obtained with 413-nm excitation are shown in Figures 8 and 9. Their ^{13}C -sensitive $\nu(\text{Fe}-\text{CO})$ modes are observed at 533 and 501 cm^{-1} , respectively. As seen in Figures 8 and 9, these peaks are clearly absent in the spectra of the parent 5-coordinate compounds, Fe(OEC)(THF) and Fe(DC)(2-MeIm). The CO stretching mode of the Fe(OEC)(THF)(CO) complex was again observed in both FT-IR and rRaman spectra at $\sim 1953 \text{ cm}^{-1}$ (1916 cm^{-1} with ^{13}CO) (Table 2). The corresponding values for Fe(DC)(2-MeIm)(CO) are 1959 cm^{-1} (FT-IR) and 1961 cm^{-1} (rRaman), with a ^{13}CO isotope shift of $\sim 40 \text{ cm}^{-1}$ (Table 2). The $\delta(\text{Fe}-\text{C}-\text{O})$ modes of these two chlorin-CO complexes were not apparent.

The present study provides the first examples of Fe-CO frequencies of metallochlorin-CO complexes. Infrared CO frequencies of related chlorin complexes have been previously reported and were known to be similar to those of the corresponding metalloporphyrin complexes.³⁶ These data are summarized in Table 2. Interestingly, these $\nu(\text{CO})$ values lie within 10 cm^{-1} of each other in the range 1951–1961 cm^{-1} . Clearly, the CO stretch alone is not very sensitive to the nature of the opposite ligand, whereas the Fe-CO frequencies respond significantly to the identity of the fifth ligand. A $\nu(\text{CO})$ vs $\nu(\text{Fe}-\text{CO})$ plot exhibits sets of lines that group according to the identity of the fifth ligand (Figure 10), as discussed in the following section. This study shows that the correlation may

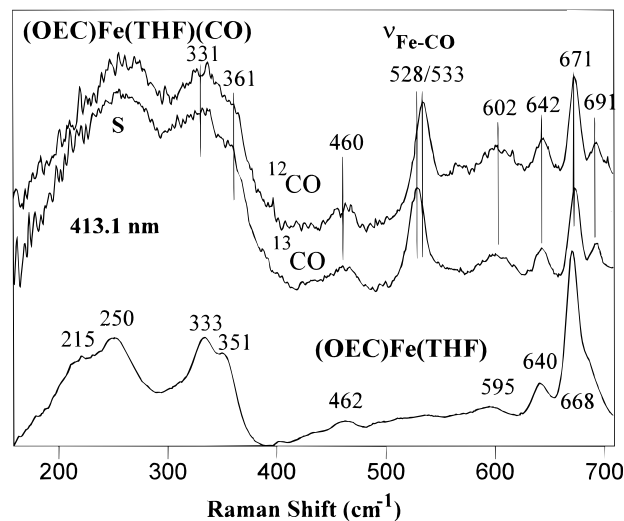


Figure 8. Low-frequency resonance Raman spectra of Fe(OEC)(THF)(CO) and Fe(OEC)(THF) obtained with 413.1-nm excitation. The laser power was 10 mW for Fe(OEC)(THF) and 2 mW for its CO complex. The spectra of ^{12}CO and ^{13}CO samples were collected back-to-back under identical instrumental conditions.

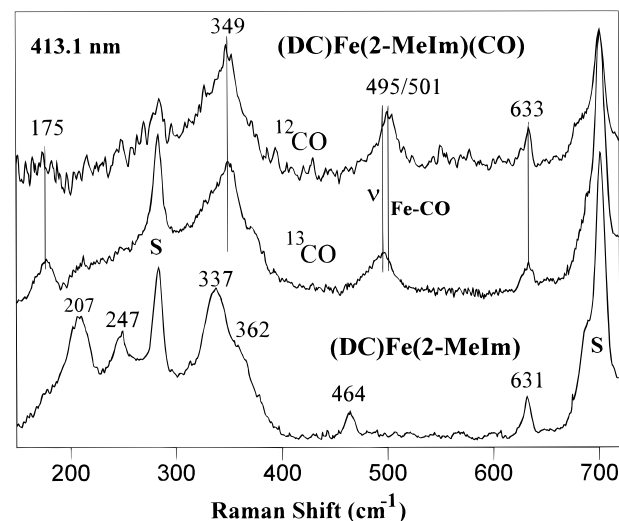


Figure 9. Low-frequency resonance Raman spectra of Fe(DC)(2-MeIm)(CO) and Fe(DC)(2-MeIm) obtained with 413.1-nm excitation. The laser power was 10 mW for Fe(DC)(2-MeIm) and 0.5 mW for its CO complex. The spectra of ^{12}CO and ^{13}CO samples were collected back-to-back under identical instrumental conditions.

TABLE 2: Fe-CO and CO Stretching Frequencies of CO Complexes of Ferrous Chlorins

compounds	$\nu(\text{Fe}-\text{CO})$ Raman	$\nu(\text{CO})$		ref
		Raman	IR	
Fe(OEC)(2-MeIm)(CO)	506	1957	1954	this work
Fe(OEC)(<i>N</i> -MeIm)(CO)			1956	ref 36
Fe(OEC)(py)(CO)			1961	ref 36
Fe(DC)(2-MeIm)(CO)	501	1961	1959	this work
Fe(OEC)(THF)(CO)	533	~ 1953	~ 1953	this work
Fe(OEC)(CO)			1951	ref 36

be extended to chlorin systems and may be of considerable utility in biological studies where the proximal ligation of chlorin *d* cofactors are yet to be established.

D. Extension of Porphyrin $\nu(\text{CO})$ vs $\nu(\text{Fe}-\text{CO})$ Plot to Chlorin Systems. CO adducts of heme proteins and model compounds have been studied extensively by rRaman spectroscopy. It was found that a $\nu(\text{CO})$ vs $\nu(\text{Fe}-\text{CO})$ graph exhibits an inverse linear relationship that reflects the π -back-bonding interactions between the iron $e_g(d_{xz}, d_{yz})$ and the CO π^*

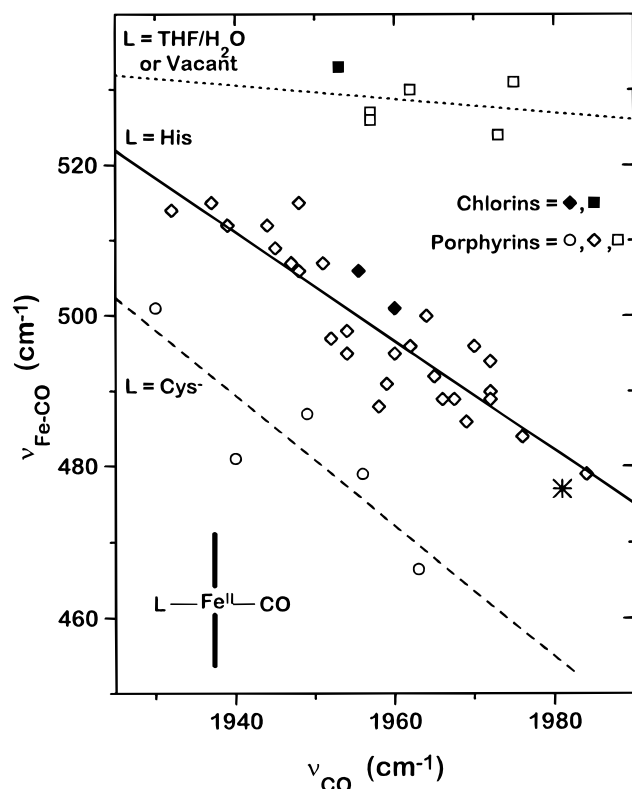


Figure 10. $\nu(\text{CO})$ vs $\nu(\text{Fe-CO})$ plots of CO complexes of ferrous porphyrins and chlorins. The porphyrin data are from Table 1 of ref 25. The dotted line (top) is a linear regression fit to the data for compounds 1–5 in ref 25 and $\text{Fe}(\text{OEC})(\text{THF})(\text{CO})$ from the present study. The solid line (middle) is the linear regression to the data for compounds 7–32 and 34 in ref 25. The data for $\text{Fe}(\text{OEC})(2\text{-MeIm})(\text{CO})$ and $\text{Fe}(\text{DC})(2\text{-MeIm})(\text{CO})$ from the present study are also included in this fit. The dashed line (bottom) is the linear regression to the data for compounds 35–37 in ref 25 and two forms of NO synthase from ref 48. The three sets of compounds are distinct in having different proximal ligands as indicated. The asterisk is from data for cytochrome *bd* oxidase taken from ref 41.

orbitals.^{22–25} For a given proximal ligand (e.g., imidazole), increased back-bonding arising from environmental effects raises $\nu(\text{Fe-CO})$ but lowers $\nu(\text{CO})$. Such environmental effects include solvent, polarity, and H-bonding interactions in both the proximal and distal regions. The CO and Fe-CO frequencies for a series of iron porphyrin complexes and heme proteins are linearly correlated with a negative slope for species possessing the same proximal ligand (Figure 10). In this diagram, the line for porphyrins with a weak or absent fifth ligand (5cHS or 6cHS with THF or water) is located above the imidazole/histidine correlation, which, in turn, lies above the thiolate/cysteine correlation, reflecting the order of increasing electron-donating ability of the fifth ligand and its dominant trans effect.

In iron chlorins, the balance between equatorial and axial π -back-bonding is similar to that of iron porphyrins, as discussed in section A, and thus, it is expected that the proximal ligand can modulate $\nu(\text{Fe-CO})$ and $\nu(\text{CO})$ to the same extent as in iron porphyrins. To our knowledge, however, this has not previously been tested for carbon monoxide complexes of iron chlorins. Indeed, the data obtained in this study meet that expectation perfectly, as shown in Figure 10 by the three solid symbols. $\text{Fe}(\text{OEC})(2\text{-MeIm})(\text{CO})$ and $\text{Fe}(\text{DC})(2\text{-MeIm})(\text{CO})$ lie on the imidazole ($L = \text{His}$) correlation line, and $\text{Fe}(\text{OEC})(\text{THF})(\text{CO})$ lies on the line for iron porphyrins with weak proximal ligands. Hence, we are confident that the correlations for the iron porphyrins can be extended to iron chlorin systems

and may provide a meaningful way to establish the proximal ligand of the iron chlorin complexes and heme *d* proteins.

As an example of the utility of the technique, recent data available for a CO adduct of cytochrome *bd* oxidase are re-evaluated. CO and Fe-CO frequencies of 1981 and 477 cm^{-1} are available from FT-IR and rRaman experiments, respectively.^{41,42} The FT-IR value of $\nu(\text{CO})$ obtained at 10 °C agrees well with the 1984- cm^{-1} value reported for a 20 K experiment.⁴³ These frequencies allow one to place a cytochrome *bd* oxidase data point (asterisk) on the correlation plot (Figure 10). Interestingly, this point falls near the extreme of the $L = \text{His}$ line. Taken at face value, this point would suggest that the chlorin *d* cofactor is ligated to a histidine, possibly one in an unusual environment.⁴¹

Extensive studies from our laboratories on cytochrome *bd* oxidase, however, suggest that the iron in the chlorin cofactor is either only very weakly coordinated or has no proximal protein ligand at all.^{14,15} Our own attempts to measure $\nu(\text{Fe-CO})$ have been unsuccessful owing to the extreme photolability of the adduct. Hill and co-workers showed that the photodissociated CO can migrate and bind to the iron of the nearby heme *b*₅₉₅, where it exhibits a different CO frequency of $\sim 1975 \text{ cm}^{-1}$.⁴³ This *b* heme has been shown to be coordinated to a histidine axial ligand.¹⁵ We suggest, therefore, that the data point representing cytochrome *bd* oxidase on Figure 10 may be from the species in which CO is bound to the normally 5cHS cytochrome *b*₅₉₅ rather than to the chlorin *d* cofactor.

Conclusions

Resonance Raman data on ferrous chlorins and their CO complexes have shown the following.

(1) Soret and Q_y spectra are dominated by polarized bands, indicating an A-term (Franck-Condon) enhancement mechanism. The iron spin and ligation indicator bands ν_3 and ν_{10} are intense with Soret excitation; the latter can still be clearly observed with Q_y excitation in which ν_3 is weak. The frequencies of ν_3 and ν_{10} are almost identical to those of porphyrins.

(2) The skeletal mode frequencies of the ferrous chlorin samples change in the CO-bound chlorins in a manner that exactly parallels the behavior of iron porphyrins. For chlorin-CO complexes, $\nu(\text{Fe-CO})$, $\nu(\text{CO})$, and $\delta(\text{Fe-C-O})$ are enhanced by both Soret and Q_y excitation via an A-term mechanism. We suggest that axial ligand vibrational modes can be observed with Q_y excitation if they are enhanced in Soret excitation. This situation may apply to other heme systems with reduced molecular symmetry such as verdohemes and bacteriochlorophylls.^{44,45}

(3) The negative linear $\nu(\text{CO})$ vs $\nu(\text{Fe-CO})$ plots derived from CO complexes of hemes and iron porphyrins can be extended to iron chlorins. This finding extends the utility of this methodology to the identification of the proximal ligand of metallochlorin-containing proteins from rRaman spectral properties of their CO adducts.

Acknowledgment. This work was supported by Grant GM-34468 from the U.S. Public Health Service, National Institutes of Health. Instrumentation in the laser Raman spectroscopy laboratory at OGI was purchased with funds from shared instrumentation grants from the NIH (RR-02676) and the National Science Foundation (BIR-9216592).

References and Notes

- (1) (a) Oregon Graduate Institute of Science and Technology. (b) Michigan State University.

- (2) Timkovich, R.; Cork, M. S.; Gennis, R. B.; Johnson, P. Y. *J. Am. Chem. Soc.* **1985**, *107*, 6069–6075.
- (3) Andersson, L. A.; Sotiriou, C.; Chang, C. K.; Loehr, T. M. *J. Am. Chem. Soc.* **1987**, *109*, 258–264.
- (4) Sotiriou, C.; Chang, C. K. *J. Am. Chem. Soc.* **1988**, *110*, 2264–2270.
- (5) Kolonay, J. F., Jr.; Moshiri, F.; Gennis, R. B.; Kaysser, T. M.; Maier, R. J. *J. Bacteriol.* **1994**, *176*, 4177–4181.
- (6) Jünemann, S.; Wrigglesworth, J. M. *J. Biol. Chem.* **1995**, *270*, 16213–16220.
- (7) Murshudov, G. N.; Grebenko, A. I.; Barynin, V.; Dauter, Z.; Wilson, K. S.; Vainshtein, B. K.; Melik-Adamyanyan, W.; Bravo, J.; Ferrán, J. M.; Ferrer, J. C.; Switala, J.; Loewen, P. C.; Fita, I. *J. Biol. Chem.* **1996**, *271*, 8863–8868.
- (8) Jacob, G. S.; Orme-Johnson, W. H. *Biochemistry* **1979**, *18*, 2975–2980.
- (9) Evans, S. V.; Sishta, B. P.; Mauk, A. G.; Brayer, G. D. *Proc. Natl. Acad. Sci. U.S.A.* **1994**, *91*, 4723–4726.
- (10) Andersson, L. A.; Loehr, T. M.; Lim, A. R.; Mauk, A. G. *J. Biol. Chem.* **1984**, *259*, 15340–15349.
- (11) Andersson, L. A.; Loehr, T. M.; Chang, C. K.; Mauk, A. G. *J. Am. Chem. Soc.* **1985**, *107*, 182–191.
- (12) Ozaki, Y.; Iriyama, K.; Ogoshi, H.; Ochiai, T.; Kitagawa, T. *J. Phys. Chem.* **1986**, *90*, 6105–6112.
- (13) Kahlow, M. A.; Zuberi, T. M.; Gennis, R. B.; Loehr, T. M. *Biochemistry* **1991**, *30*, 11485–11489.
- (14) Sun, J.; Osborne, J. P.; Kahlow, M. A.; Kaysser, T. M.; Hill, J. J.; Gennis, R. B.; Loehr, T. M. *Biochemistry* **1994**, *34*, 12144–12151.
- (15) Sun, J.; Kahlow, M. A.; Kaysser, T. M.; Osborne, J. P.; Hill, J. J.; Rohlf, R. J.; Hille, R.; Gennis, R. B.; Loehr, T. M. *Biochemistry* **1996**, *35*, 2403–2412.
- (16) Andersson, L. A.; Loehr, T. M.; Sotiriou, C.; Wu, W.; Chang, C. K. *J. Am. Chem. Soc.* **1986**, *108*, 2908–2916.
- (17) Boldt, N. J.; Donohoe, R. J.; Birge, R. R.; Bocian, D. F. *J. Am. Chem. Soc.* **1987**, *109*, 2284–2298.
- (18) Prendergast, K.; Spiro, T. G. *J. Phys. Chem.* **1991**, *95*, 1555–1563.
- (19) Procyk, A. D.; Kim, Y.; Schmidt, E.; Fonda, H. N.; Chang, C. K.; Babcock, G. T.; Bocian, D. F. *J. Am. Chem. Soc.* **1992**, *114*, 6539–6549.
- (20) Kahlow, M. A.; Loehr, T. M.; Zuberi, T. M.; Gennis, R. B. *J. Am. Chem. Soc.* **1993**, *115*, 5845–5846.
- (21) Mylrajan, M.; Andersson, L. A.; Sun, J.; Loehr, T. M.; Thomas, C. S.; Sullivan, E. P., Jr.; Thomson, M. A.; Long, K. M.; Anderson, O. P.; Strauss, S. H. *Inorg. Chem.* **1995**, *34*, 3953–3963.
- (22) Uno, T.; Nishimura, Y.; Tsuboi, M.; Makino, R.; Iizuka, T.; Ishimura, Y. *J. Biol. Chem.* **1987**, *262*, 4549–4556.
- (23) Yu, N.-T.; Kerr, E. A. In *Biological Applications of Raman Spectroscopy*; Spiro, T. G., Ed.; Wiley: New York, 1988; Vol. 3, pp 39–95.
- (24) Smulevich, G.; Mauro, J. M.; Fishel, L. A.; English, A. M.; Kraut, J.; Spiro, T. G. *Biochemistry* **1988**, *27*, 5486–5492.
- (25) Ray, G. B.; Li, X.-Y.; Ibers, J. A.; Sessler, J. L.; Spiro, T. G. *J. Am. Chem. Soc.* **1994**, *116*, 162–176.
- (26) Sun, J.; Loehr, T. M.; Wilks, A.; Ortiz de Montellano, P. R. *Biochemistry* **1994**, *33*, 13734–13740.
- (27) OEC, octaethylchlorin (2,3,7,8,12,13,17,18-octaethyl-7,8-dihydro-porphyrin). Other abbreviations used are DC, deuteriochlorin; FT-IR, Fourier-transform infrared; rRaman, resonance Raman; THF, tetrahydrofuran; UV-vis, ultraviolet-visible; 2-MeIm, 2-methylimidazole. Designations for heme coordination and spin state: 5cHS, 5-coordinate high-spin; 6cLS, 6-coordinate low-spin.
- (28) Ogoshi, H.; Watanabe, E.; Yoshida, Z.; Kincaid, J.; Nakamoto, K. *Inorg. Chem.* **1975**, *14*, 1344–1350.
- (29) Loehr, T. M.; Sanders-Loehr, J. *Methods Enzymol.* **1993**, *226*, 431–470.
- (30) Strauss, S. H.; Silver, M. E.; Ibers, J. A. *J. Am. Chem. Soc.* **1983**, *105*, 4108.
- (31) Fonda, H. N.; Oertling, W. A.; Salehi, A.; Chang, C. K.; Babcock, G. T. *J. Am. Chem. Soc.* **1990**, *112*, 9497–9507.
- (32) Procyk, A. D.; Bocian, D. F. *Annu. Rev. Phys. Chem.* **1992**, *43*, 465–496.
- (33) Scheer, H.; Inhoffen, H. H. In *The Porphyrins*; Dolphin, D., Ed.; Academic Press: New York, 1979; Vol. II, pp 45–90.
- (34) Spangler, D.; Maggiora, G. M.; Shipman, L. L.; Christofferson, R. E. *J. Am. Chem. Soc.* **1977**, *99*, 7478–7489.
- (35) Gouterman, M. In *The Porphyrins*; Dolphin, D., Ed.; Academic Press: New York, 1978; Vol. III, pp 1–165.
- (36) Stolzenberg, A. M.; Strauss, S. H.; Holm, R. H. *J. Am. Chem. Soc.* **1981**, *103*, 4763–4778.
- (37) Ozaki, Y.; Iriyama, K.; Ogoshi, H.; Ochiai, T.; Kitagawa, T. *J. Phys. Chem.* **1986**, *90*, 6113–6118.
- (38) Andersson, L. A.; Mylrajan, M.; Loehr, T. M.; Sullivan, E. P., Jr.; Strauss, S. H. *New J. Chem.* **1992**, *16*, 569–576.
- (39) Yu, N. T.; Kerr, E. A.; Ward, B.; Chang, C. K. *Biochemistry* **1983**, *22*, 4534–4540.
- (40) Hirota, S.; Ogura, T.; Shinzawa-Itōh, K.; Yoshikawa, S.; Nagai, M.; Kitagawa, T. *J. Phys. Chem.* **1994**, *98*, 6652–6660.
- (41) Tsubaki, M.; Uno, T.; Hori, H.; Mogi, T.; Nishimura, Y.; Anraku, Y. *FEBS Lett.* **1993**, *335*, 13–17.
- (42) Hirota, S.; Mogi, T.; Anraku, Y.; Gennis, R. B.; Kitagawa, T. *Biospectroscopy* **1995**, *1*, 305–311.
- (43) Hill, J. J.; Alben, J. O.; Gennis, R. B. *Proc. Natl. Acad. Sci. U.S.A.* **1993**, *90*, 5863–5867.
- (44) Matera, K. M.; Takahashi, S.; Fujii, H.; Zhou, H.; Ishikawa, K.; Yoshimura, T.; Rousseau, D. L.; Yoshida, T.; Ikeda-Saito, M. *J. Biol. Chem.* **1996**, *271*, 6618–6624.
- (45) Palaniappan, V.; Aldema, M. A.; Frank, H. A.; Bocian, D. F. *Biochemistry* **1992**, *31*, 11050–11058.
- (46) Tsubaki, M.; Srivastava, R. B.; Yu, N. T. *Biochemistry* **1982**, *21*, 1132–1140.
- (47) Choi, S.; Spiro, T. G.; Langry, K. C.; Smith, K. M.; Budd, D. L.; La Mar, G. N. *J. Am. Chem. Soc.* **1982**, *104*, 4345–4351.
- (48) Wang, J.; Wu, C.; Ghosh, D. K.; Zhang, J.; Stuehr, D. J.; Rousseau, D. L. In *Proceedings of the 15th International Conference on Raman Spectroscopy*; Asher, S. A., Stein, P., Eds.; John Wiley & Sons: Chichester, U.K., 1996; Vol. I, pp 440–441.